Available online at www.sciencedirect.com
SCIENCE DIRECT®
Journal of Magnetic Resonance 167 (2004) 273–281
JMR Journal of Magnetic Resonance
www.elsevier.com/locate/jmr

Internal dynamics of hydroxymethyl rotation from CH_2 cross-correlated dipolar relaxation in methyl-β-D-glucopyranoside☆

Katalin E. Kövér,[a] Gyula Batta,[b] Jozef Kowalewski,[c,*] Leila Ghalebani,[c] and Danuta Kruk[c]

[a] Department of Inorganic and Analytical Chemistry, University of Debrecen, Egyetem tér 1, H-4010 Debrecen, Hungary
[b] Research Group for Antibiotics of the Hungarian Academy of Sciences, University of Debrecen, Egyetem tér 1, H-4010 Debrecen, Hungary
[c] Physical Chemistry, Arrhenius Laboratory, Stockholm University, S-106 91 Stockholm, Sweden

Received 10 September 2003; revised 29 December 2003

Abstract

Conventional relaxation parameters (T_1^{-1}, T_2^{-1}, and NOE), obtained at different temperatures and magnetic fields, are reported for the hydroxymethyl (C6) carbon in methyl-β-D-glucopyranoside in a D_2O/DMSO cryosolvent. These data are interpreted with the Lipari–Szabo model. In addition, two-field measurements of longitudinal and spin-locked relaxation rates related to the cross-correlated carbon–proton dipole–dipole interactions for the same carbon are reported. The complete data set consisting the conventional and cross-correlated relaxation parameters is interpreted using a new "hybrid" approach, in which the Lipari–Szabo model for the auto-correlated spectral densities is combined with the two-site jump model for the cross-correlated spectral densities, with the global correlation time as a common parameter. The two-site jump rates thus obtained are in reasonable agreement with the ultrasonic relaxation measurements, and have reasonable temperature dependence.

1. Introduction

Cross-correlation or interference phenomena in NMR relaxation have been known for long time [1–5], but the interest in studying these processes has increased dramatically during the recent decade, as it has been realized that they are an invaluable source of both dynamic and structural information [6–8]. In analogy with many other development trends in NMR, the interest in cross-correlation effects is driven to a large extent, but not exclusively, by the possibilities they open for studies of biological macromolecules [9–14].

Briefly, the interference relaxation phenomena arise as a result of the simultaneous presence of two interactions in the Hamiltonian, H_1, leading to nuclear spin relaxation (if more than two terms are present, several pairwise interference terms can occur). The necessary condition for the interference effects to occur is that the interactions have the same tensor rank and that the stochastic processes modulating them are correlated in a statistical sense. This last fact is the reason for the concepts of interference and cross-correlation being used more or less as synonyms. Let us consider a perturbation Hamiltonian consisting of two such terms, H_A and H_B:

$$H_1 = H_A + H_B \tag{1}$$

H_1 can be represented as a matrix in an arbitrary Hilbert space and the matrix elements $(H_1)_{\alpha\beta}$ will be equal to the sums of matrix elements of H_A and H_B . The expressions for relaxation rate constants always contain squares of matrix elements of H_1; these can be expressed as:

$$((H_1)_{\alpha\beta})^2 = ((H_A)_{\alpha\beta})^2 + ((H_B)_{\alpha\beta})^2 + 2(H_A)_{\alpha\beta}(H_B)_{\alpha\beta}. \tag{2}$$

The cross-correlation effects arise from the last term of Eq. (2). In the relaxation expressions, it is multiplied by the cross-correlation spectral density, i.e., the Fourier transform of the time cross-correlation function. The latter quantity describes the extent of temporal correlation of the stochastic processes modulating H_A and H_B [6–8]. The most commonly studied interference phenomena are those related to the intramolecular rank-two interactions, the dipole–dipole (DD) interaction,

☆ This work has been presented in part at the EENC, Prague, 2002.
* Corresponding author. Fax: +46-8-15-21-87.
E-mail address: jk@physc.su.se (J. Kowalewski).

1090-7807/$ - see front matter © 2004 Elsevier Inc. All rights reserved.
doi:10.1016/j.jmr.2004.01.003

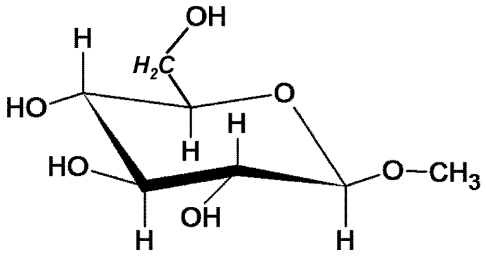

Scheme 1. Me-β-D-glucopyranoside.

the chemical shielding anisotropy (CSA), and the quadrupolar (Q) interaction. All these interactions are sources of relaxation in liquid solutions, because the molecular tumbling reorients their principal axes with respect to the external field [15,16].

The extent of the cross-correlation between pairs of interactions mentioned above depends, on the one hand, on the interaction strengths and the relative orientation of the principal axes and, on the other hand, on the details of the reorientational processes. The former property is the origin of the structural information present in the cross-correlated relaxation rates (abbreviated below as CCRR), while the latter has the potential of providing new dynamical information. In this work we concentrate on the case of a methylene group and the cross-correlation between the two carbon-proton dipolar interactions present there. The geometry of methylene groups—and thus the strengths and relative orientations of the interactions—can in most cases be assumed known. Therefore, it is easy to concentrate on obtaining the dynamical information. This information is also, in many common situations, highly interesting because the methylene groups can be expected to undergo other motions than reorientation of the molecule as a whole. In fact, several groups have used a similar approach before [4,9,17–25]. Here we study the exocyclic hydroxymethyl group (CH_2OH) in a simple carbohydrate, methyl-β-D-glucopyranoside (Me-β-D-glcp), scheme 1. The hydroxymethyl groups in sugars are known to undergo internal motions [26–29], but the details of the dynamic processes involved are far from clear. This made us interested in testing the applicability of the CCRR measurements as a source of further information on these dynamic processes. Such measurements allow, in addition, estimating rotamer populations without referring to the Karplus curves.

The layout of the paper is as follows: Section 2 covers the experimental details and Section 3 describes the theory. The results are presented and discussed in Section 4 and the conclusions are drawn in Section 5.

2. Experimental

Me-β-D-glcp, selectively carbon-13 labeled in the hydroxymethyl group, was synthesized according to Herzig and co-workers [30,31]. The solvents D_2O and DMSO-d_6 were obtained from Aldrich and used without further purification. Approximately 40 mg of Me-β-D-glcp was dissolved in a 7:3 molar ratio mixture of D_2O and DMSO-d_6, to give about 0.4 M solution. The solution was transferred to a 5 mm NMR tube and sealed under vacuum after removal of the dissolved oxygen through three freeze–pump–thaw cycles.

Most NMR experiments were performed at 9.4 Tesla using a Varian Inova 400 spectrometer and at 11.8 T with a Bruker Avance DRX 500 spectrometer. A Varian Inova 600 spectrometer operating at 14.1 T was also used in some cases. All the experiments were performed using standard variable temperature controllers provided by the instrument manufacturers. The temperature was calibrated with a methanol chemical shift thermometer [32]. Deuterium lock for field/frequency stabilization was used in all experiments.

A modified 5 mm carbon-13 probehead from Jeol was used on the 9.4 T instrument, a triple-resonance HCP probehead was used on the Inova 600, while a Bruker inverse-detection 5 mm broadband probehead was used on the 11.8 T spectrometer. The carbon-13 spin–lattice relaxation time (T_1) was measured by the inversion-recovery method with 10–12 different delays. The nuclear Overhauser enhancements (NOE) were determined by the dynamic NOE (DNOE) technique [33] with one long (about 5 T_1) and one short (about 1 ms) delay, or simply by gated decoupling. The NOE factor, $1+\eta$, is expressed as the intensity ratio of the enhanced signal (long delay in the DNOE experiment) to the unenhanced signal (short delay). The spin–lattice relaxation time in a rotating frame ($T_{1\rho}$) was measured with a spin-lock field of 0.8 kHz placed on resonance. In the absence of chemical exchange on the microsecond timescale, $T_{1\rho}$ should be equivalent to T_2 [16]. A recycle delay of about 5 times the longest T_1 was used in the inversion-recovery and spin-lock experiments, whereas it was about $10T_1$ in the NOE experiments. Broadband proton decoupling was carried out by the Waltz-16 scheme with a typical 90° decoupler pulse duration of about 100–150 μs. A line broadening of 2–4 Hz was applied before evaluating line intensities. The three-parameter exponential fitting routine provided by the instrument manufacturers was used to evaluate the spin–lattice relaxation rate and a two-parameter fitting routine was used in the $T_{1\rho}$ measurements. The carbon-13 90° pulse duration was about 7 μs at 9.4 T, 14.5 μs at 14.1 T, and about 16 μs at 11.8 T. The spectral width was typically around 50 ppm, the number of data points was about 8 K and the number of transients 4–32. The accuracy of the T_1, $T_{1\rho}$, and NOE data is estimated to be better than 3, 3, and 5%, respectively. All the experiments were repeated at least twice, and average values are reported.

Cross-correlation rates were measured by the modified sequences of Kövér and Batta [34]. The pulse

schemes designed for quantitative measurement of longitudinal (Fig. 1A) and transverse (Fig. 1B) dipole–dipole cross-correlated relaxation rates (DD/DD CCRR) have been treated in detail elsewhere [34]; therefore we will give only a concise description here. The one-dimensional DD/DD cross-correlation experiments depicted in Fig. 1 are suitable for accurate measurement of fairly weak interference effects in small-to-medium sized molecules. The longitudinal (laboratory frame) experiment of Fig. 1A monitors the build-up of three-spin order, $\langle 4I_{1z}I_{2z}S_z\rangle$, from the inverted carbon magnetization exclusively through relaxation interference between the CH^1/CH^2 dipolar interactions of the methylene CH_2 group (where $I = {}^1H$, $S = {}^{13}C$). The 90° carbon pulse applied after the variable delay time (t_d) transfers the *zzz* magnetization into double-antiphase carbon magnetization, $\langle 4I_{1z}I_{2z}S_y\rangle$, which will be refocused through the large proton–carbon ($^1J_{CH}$) scalar coupling with the subsequent spin-echo sequence before detection. Undesired magnetization components (such as the strong antiphase and weak in-phase carbon terms) arising from the huge residual carbon $\langle S_z\rangle$ magnetization after t_d can be eliminated by broadband proton decoupling and difference-mode acquisition, respectively. This procedure is similar to that proposed by Jaccard et al. [35] for the case of longitudinal two-spin order. Accordingly, the proton 90° pulse (striped bar in Fig. 1) applied for the second 16 transients converts the desired *zzz* magnetization into unobservable multiple quantum coherence, while leaving the undesired magnetizations unaffected, which allows their perfect cancellation in the difference experiment. As a result, the initial build-up rate of the detected carbon signal will be proportional to the longitudinal cross-correlation rate, $\Gamma^{\text{long}}_{\text{CH,CH}}$. The initial magnetization state can be quantified in a reference experiment using the pulse scheme of Fig. 1A, with t_d of 3 μs and discarding the proton 180° pulse from the subsequent spin-echo sequence.

The transverse (rotating frame) cross-correlation experiment of Fig. 1B measures the build-up of double-antiphase carbon magnetization, $\langle 4I_{1z}I_{2z}S_y\rangle$, during a continuous-wave spin-lock pulse of variable duration (V_{SL}). Relaxation interference between the CH^1/CH^2 dipoles of CH_2 group is the only source of the conversion of carbon $\langle S_y\rangle$ magnetization to $\langle 4I_{1z}I_{2z}S_y\rangle$. The initial build-up of the interference signal is proportional to the transverse cross-correlation rate, $\Gamma^{\text{spin-lock}}_{\text{CH,CH}}$. Contributions from the undesired coherences are removed as detailed above in the longitudinal experiment using proton decoupling and difference mode during acquisition. In the following we refer to these experiments as "decoupled difference experiments."

The CCRRs were evaluated as initial rates. Second-order polynomials were fitted to the initial part of the build-up curve, and the derivative at time zero was obtained from the polynomial. The uncertainty of the cross-correlated relaxation rates is estimated at about 15%. The variable-field relaxation data were analyzed with MATLAB [36] running on a PC. The Monte-Carlo error analysis was accomplished by adding random

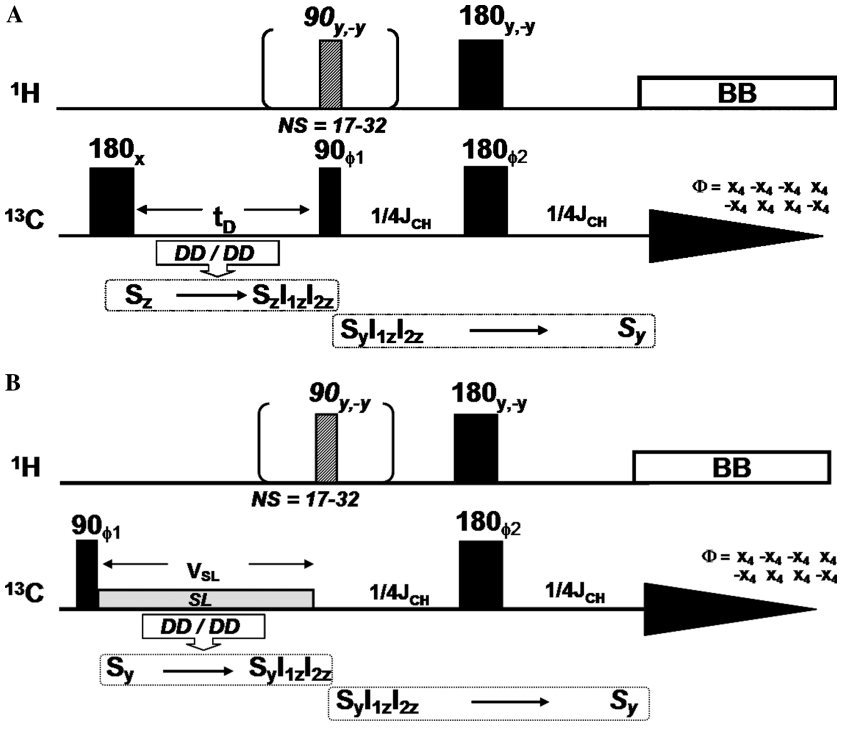

Fig. 1. Pulse sequences used for determination of cross-correlated relaxation rates. For details see Section 2.

noise to the data within experimental uncertainties, and repeating the fits 250 times. In some cases, we also carried out simple proton-coupled carbon-13 inversion-recovery experiments. The carbon pulses and the spectral width were the same as in the "conventional" measurements, but the number of transients was somewhat larger (typically 64–128).

3. Theory

The theory of NMR relaxation, including cross-correlated relaxation, is well understood, and we limit ourselves here to the presentation of relevant equations. For an aliphatic, proton-bearing carbon-13 spin, one can usually neglect other relaxation mechanisms than the dipolar interaction with directly bonded protons (such as the chemical shielding anisotropy, CSA). The "standard" relaxation parameters, T_1^{-1}, T_2^{-1}, and NOE are then given by [37]:

$$T_1^{-1} = \frac{n_H}{10} D_{CH}^2 [J_{CH}(\omega_H - \omega_C) + 3J_{CH}(\omega_C) + 6J_{CH}(\omega_H + \omega_C)], \tag{3}$$

$$T_2^{-1} = T_{1\rho}^{-1} = \frac{n_H}{20} D_{CH}^2 [4J_{CH}(0) + J_{CH}(\omega_H - \omega_C) + 3J_{CH}(\omega_C) + 6J_{CH}(\omega_H) + 6J(\omega_H + \omega_C)], \tag{4}$$

$$\eta = \left(\frac{\gamma_H}{\gamma_C}\right) \frac{6J_{CH}(\omega_H + \omega_C) - J_{CH}(\omega_H - \omega_C)}{J_{CH}(\omega_H - \omega_C) + 3J_{CH}(\omega_C) + 6J_{CH}(\omega_H + \omega_C)}, \tag{5}$$

where n_H is the number of protons directly bonded to the carbon ($n_H = 2$ for a methylene group), D_{CH} is the carbon–proton dipole–dipole coupling constant, $D_{CH} = \frac{\mu_0 \gamma_C \gamma_H \hbar}{4\pi\, r_{CH}^3}$ (where r_{CH} is the carbon–proton bond distance), and $J_{CH}(\omega)$ is the carbon–proton dipolar auto-correlation function. Eq. (5) assumes that the NOE is not affected by the presence of cross-correlation effects. This is valid as long as the proton system does not possess any symmetry [38].

Using the common Lipari–Szabo approach, the spectral density takes the form [39]:

$$J_{CH}(\omega) = \frac{S_{CH}^2 \tau_M}{1 + \omega^2 \tau_M^2} + \frac{(1 - S_{CH}^2)\tau}{1 + \omega^2 \tau^2}, \tag{6}$$

where $\tau^{-1} = \tau_M^{-1} + \tau_e^{-1}$, τ_M is a correlation time for the global motion, common to the whole molecule, τ_e is the correlation time for the fast local motion, specific for every individual site in the molecule, and S_{CH} is the generalized order parameter for the CH axis. S_{CH} reflects the spatial restriction of the local motion. Note that the spectral density is normalized in a slightly different way than the usual form. Expressions for the spectral density for a variety of models, allowing for overall rotation and an internal motion of a specified kind, are also available in the literature [9]. For the case of the hydroxymethyl group in carbohydrates, the two-site jump model is of particular interest (vide infra). The expression for the auto-correlation spectral densities in this model is:

$$J_{CH}(\omega) = \frac{S_j^2 \tau_M}{1 + \omega^2 \tau_M^2} + \frac{(1 - S_j^2)\tau}{1 + \omega^2 \tau^2} \tag{7}$$

with

$$S_j^2 = 1/9 + 8/27(1 - 4P(1 - P)\sin^2\gamma) + 16/27(1 - 4P(1 - P)\sin^2 2\gamma) \tag{8}$$

and $\tau^{-1} = \tau_M^{-1} + \tau_j^{-1}$.The symbol τ_j is the inverse jump rate, P is the population of one of the rotamers, and γ is the jump half-angle (the jumps are between $+\gamma$ and $-\gamma$). The coefficients in the expression for auto-correlation order parameters, S_j^2, are based on the tetrahedral HCH angle; a more general expression has been given in the literature [9]. In the case of an "ideal" two-site jump ($P = 0.5$ and $\gamma = \pm 60°$) Eq. (8) would yield $S_j^2 = 0.333$.

We can note that the structure of the spectral densities in the two approaches is the same. However, an important difference is that the S_j^2-parameter of the jump model is related to the more basic parameters of that model.

In addition to the standard relaxation parameters, we have measured two types of cross-correlated relaxation rates, which are related to the dipolar interaction strengths and dynamic parameters according to [4,20]:

$$\Gamma_{CH,CH}^{long} = \frac{3}{5} D_{CH}^2 K_{HCH}(\omega_C), \tag{9}$$

$$\Gamma_{CH,CH}^{spin\text{-}lock} = \frac{3}{10} D_{CH}^2 \left[\frac{4}{3} K_{HCH}(0) + K_{HCH}(\omega_C)\right], \tag{10}$$

where

$$K_{HCH}(\omega) = \frac{Q_j^2 \tau_M}{1 + \omega^2 \tau_M^2} - \frac{\left(1/3 + Q_j^2\right)\tau}{1 + \omega^2 \tau^2} \tag{11}$$

with

$$Q_j^2 = 1/9 - 4/27(1 - 4P(1 - P)\sin^2\gamma) - 8/27(1 - 4P(1 - P)\sin^2 2\gamma) \tag{12}$$

and $\tau^{-1} = \tau_M^{-1} + \tau_j^{-1}$.

The two CCRRs refer to the transfer of longitudinal carbon-Zeeman order into the three-spin order and the corresponding transfer under carbon-spin-lock conditions. The cross-correlation spectral densities, $K_{HCH}(\omega)$, refer to the interference between the two CH dipolar interactions. The coefficients in Eq. (12) are also based on the tetrahedral HCH angle. In this case, the "ideal" two-site jump model results in the cross-correlation order parameter $Q_j^2 = 0$. It should be stressed that, while the longitudinal CCRR depends only on the cross-correlated spectral density at the carbon-13 Larmor

frequency, the rotating-frame CCRR also carries information on the zero-frequency spectral density. This is important outside of the extreme narrowing regime.

The counterpart of the "model-free" Lipari–Szabo approach to the cross-correlation spectral densities has also been formulated [40–42]. Instead of the generalized order parameter, the expression contains another quantity, defined in terms of products of mean values of spherical harmonics describing the orientations of the two principal axes. As discussed by Daragan and Mayo [9], one can find relations between these parameters and S^2_{CH} for specific dynamic models. Following Chenon and Werbelow [25], we choose not to use the "model-free" approach in the case of cross-correlated spectral densities.

4. Results and discussion

The relaxation rates determined at two (sometimes three) fields and four temperatures are summarized in Table 1. We can notice, from the inequality of T_1^{-1} and $T_{1\rho}^{-1}$, and from the NOE being lower than 2.99, that the motion of Me-β-D-glcp is outside of extreme narrowing even at the highest temperature. This is caused by the high viscosity of the solvent mixture [29]. As opposed to T_1^{-1} and $T_{1\rho}^{-1}$, the CCRRs can have either sign and—as we can see in the Table 1—are in all cases measured as negative.

In Fig. 2 we show a typical set of spectra from the decoupled difference CCRR experiment consisting of a carbon inversion followed by the detection of the three-spin order. The build-up of the longitudinal three-spin order can also be followed by a simple carbon inversion-recovery experiment without proton decoupling. The advantage of the inversion-recovery experiment is its simplicity and the fact that the sign of the resulting three-spin order (expressed as a difference between the summed intensity of the outer lines minus the central line) can easily be established without ambiguity. In the decoupled difference experiments, we can with ease determine the relative signs of the longitudinal and the spin-lock rates, while the determination of the absolute sign of the CCRRs is somewhat more difficult. For quantification of the initial rate we believe, however, that the decoupled difference experiments are more suitable. In Fig. 3 we show the build-up of the interference signals obtained from both types of decoupled difference experiments.

Table 1
Relaxation rates for the hydroxymethyl group in Me-β-D-glcp

Temperature (K)	Magnetic field (T)	$2(T_1)^{-1}$	$2(T_{1\rho})^{-1}$	$1+\eta$	$\Gamma^{\text{long}}_{\text{CH, CH}}$	$\Gamma^{\text{spin-lock}}_{\text{CH, CH}}$
263	9.4	4.37	7.7	1.35	−1.81	−2.70
	11.75	3.48	6.4	1.39	−1.63	−2.42
277	9.4	4.06	4.63	1.71	−1.11	−1.24
	11.75	3.40	4.46	1.63	−1.18	−1.35
	14.1	2.94		1.48		
284	9.4	3.65	4.00	1.96	−0.84	−0.80
	11.75	3.07	3.74	1.85	−0.91	−1.00
	14.1	2.73		1.70		
300	9.4	2.63	2.82	2.50	−0.35	−0.40
	11.75	2.28	2.53	2.42	−0.39	−0.35

All rates are in s^{-1}; $1+\eta$ is dimensionless. Estimated uncertainties are about ±3% for T_1^{-1}, $T_{1\rho}^{-1}$, and ±5% for $1+\eta$, and about ±15% for the cross-correlated rates.

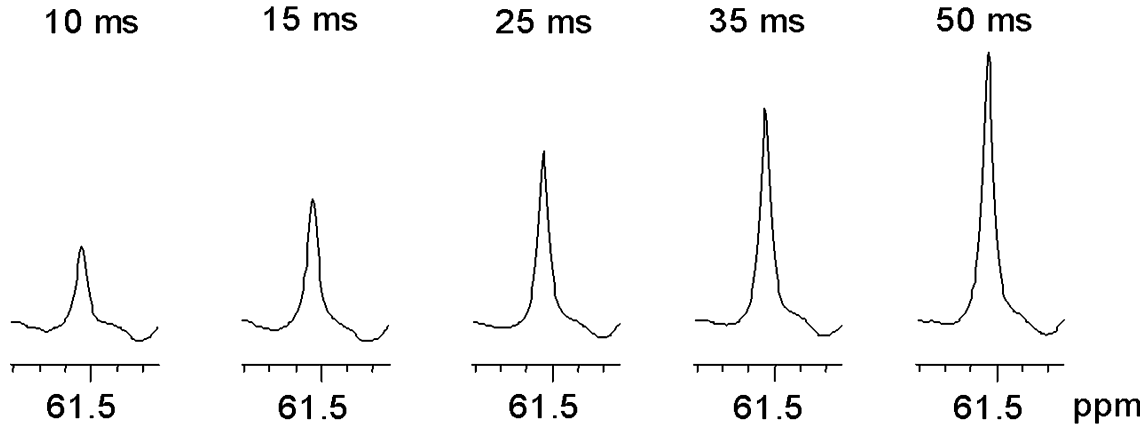

Fig. 2. A typical set of experimental spectra from the longitudinal decoupled difference CCRR experiment. Data are obtained at 11.75 T and 277 K.

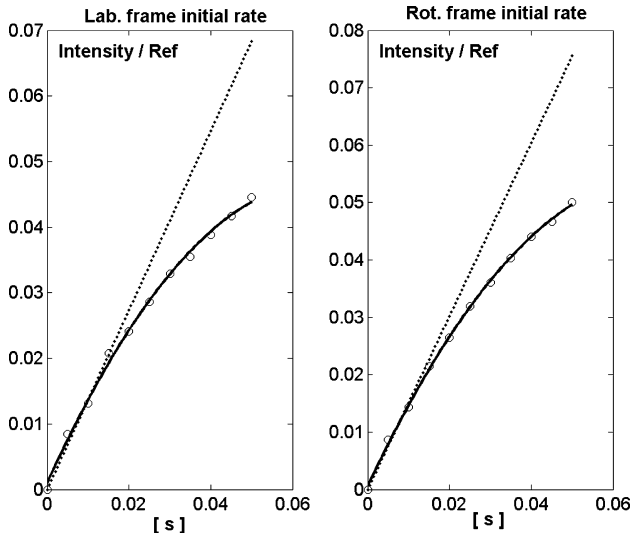

Fig. 3. An example of initial-rate determination from the CCRR experiments, based on the measured integrated intensities. Data are obtained at 11.75 T and 277 K.

In order to analyze the rates in Table 1 in terms of correlation times and order parameters, we adopt the following strategy. In the first step, we analyze the conventional T_1, T_2, and NOE relaxation parameters at each temperature, using the Lipari–Szabo model (Eq. (6)) and assuming the dipolar coupling constant of 21.5 kHz, corresponding to a single-bond carbon–proton distance of 112 pm [43–45]. Fitting the Lipari–Szabo parameters to the six or eight rates (T_1^{-1}, $T_{1\rho}^{-1}$, and NOE at 9.4 and 11.8 T at 263 and 300 K; at 277 and 284 K, in addition T_1^{-1} and NOE at 14.1 T) yields the τ_M, S^2_{CH}, and τ_e parameters collected in Table 2. We note that the global correlation time increases with decreasing temperature, as expected. The order parameter is close to earlier results for exocyclic hydroxymethyl groups in sugars [27–29], when corrected for the different assumed CH distance. Similarly, the order parameter increases at lower temperatures, as expected. The local correlation times are less well determined, as usual, and their temperature dependence is difficult to interpret. In general, the uncertainties of the fitted parameters (obtained by Monte Carlo technique) based on the data at two fields are larger than obtained from three-field analysis. In a similar way, one can use the two-site jump model to analyze the T_1^{-1}, $T_{1\rho}^{-1}$, and NOE data. Since the structures of the spectral densities are the same, the results (not shown) of the two-site jump analysis are rather similar, as far as the resulting correlation times are concerned.

Table 2
Results of the Lipari–Szabo fitting of T_1^{-1} and $T_{1\rho}^{-1}$ and NOE data for the hydroxymethyl group in Me-β-D-glcp

Temperature (K)	S^2	τ_M (ps)	τ_e (ps)
263	0.78(0.02)	1510(73)	78(21)
277	0.69(0.07)	842(93)	83(32)
277[a]	0.79(0.04)	702(58)	28(25)
284	0.66(0.12)	604(121)	67(46)
284[a]	0.72(0.08)	546(71)	48(33)
300	0.61(0.20)	347(161)	36(46)

The numbers in parentheses are parameter uncertainties estimated by a Monte Carlo procedure.
[a] Three-field data.

In the second step of the analysis, we include the cross-correlated relaxation rates in the discussion. We note that both the laboratory frame and the spin-lock CCRRs in Table 1 are negative in all cases. Following the analysis of Ernst and Ernst [20] and assuming reasonable values of global and local dynamics for Me-β-D-glcp, we find that this might be consistent with either the two-site jump model or restricted rotational diffusion model. Following the recent work by Chenon and Werbelow [25] on the CCRRs in methylene groups in a peptide, we have selected the two-site jump model. However, it is possible that the restricted rotational diffusion model would give similar results. Theoretical CCRRs calculated for a few possible models are compared on Fig. 4. This figure suggests, that shifting the temperature can help in the selection of the appropriate motional model. The choice of the two-site (rather than three-site) model is further corroborated if we identify the two sites as two possible staggered conformations of the CH_2OH group with respect to the C5H5 bond (Fig. 5) and consider the vicinal indirect proton-proton coupling constants between proton H5 and protons H6S and H6R. These coupling constants are averages, possibly weighted with unequal populations of the two states. The measured coupling constants at 277 K are $^3J_{H\text{-}5,H\text{-}6R} = 6.4$ and $^3J_{H\text{-}5,H\text{-}6S} = 2.1$ Hz, respectively. Using the Karplus relation [46,47], we can estimate the gg, gt and tg populations as 41, 66, and −7% (the unphysical negative population refers to the third rotamer, also shown in Fig. 5). Our results measured in the binary solvent are in reasonable agreement with the work of Tvaroska et al. [48], although they measured the coupling constants in water solution.

Thus, we have attempted to analyze the full data set of the auto- and cross-correlated relaxation rates using the two-site jump model. The results (not shown) turned out to be unsatisfactory in the sense that the fit produced internal jump rates increasing with decreasing temperature. The conclusion we draw from this finding is that the fast local dynamics of the hydroxymethyl group cannot be described by a simple two-site jump model. This notion is corroborated by the observation that the values of the generalized order parameters of the Lipari–Szabo model ($S^2 = 0.52$–0.78 in Table 2) are significantly larger than 0.333 (the expected value for S_j^2 in the ideal two-site jump model).

Considering these apparently contradictory results, we propose the use of a combined dynamic model to interpret all the experimental data simultaneously. In

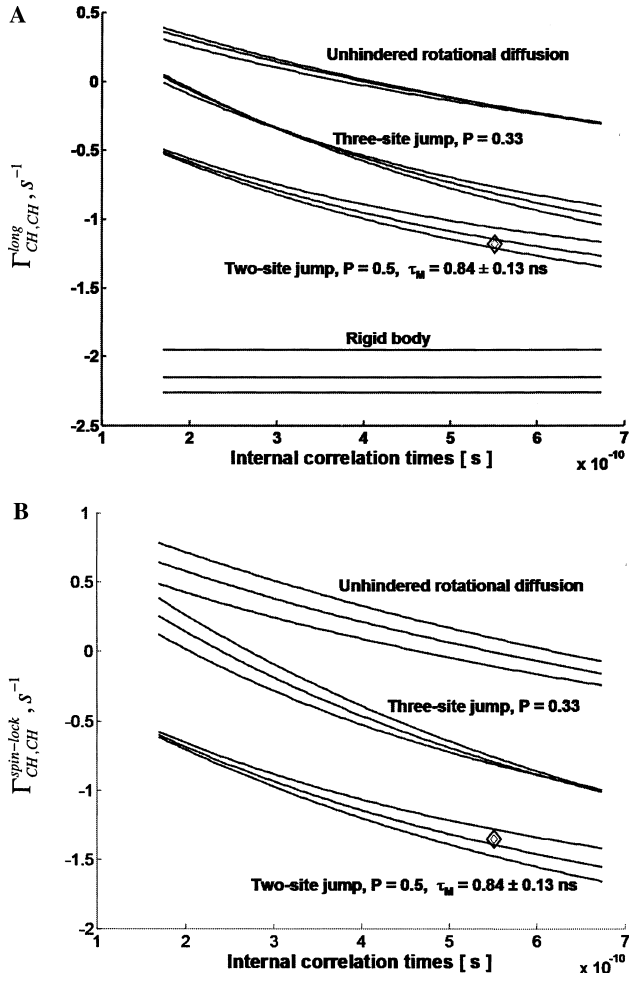

Fig. 4. Theoretical dependence of the CCRRs on the global and local correlation times using: rigid body, unrestricted rotational diffusion, and two- and three-site jump models (with equal populations and tetrahedral geometry). (A) Laboratory frame and (B) rotating frame. Triple curves represent the ±error range of the global correlation time parameter, τ_M. Experimental points measured at 277 K are labeled with diamonds. This figure illustrates that temperature dependence may help to select the appropriate motional model.

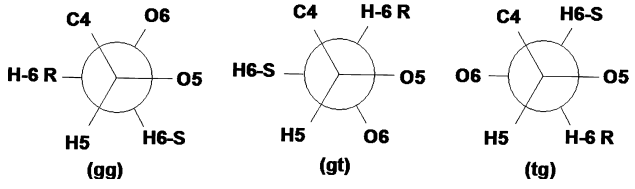

Fig. 5. The three different staggered conformations of the hydroxymethyl group.

this integrated approach we actually deal with a situation where three kinds of motion are present: the global reorientation, the conformational jumps, and the more limited fast local motions at each of the potential minima. The conventional relaxation parameters seem to be most sensitive to the global motions and to the fast local motions, while the CCRRs appear to reflect the conformational jumps.

In the proposed approach, both auto- and cross-correlated relaxation data are simultaneously analyzed: the fast internal motion is characterized by the two local Lipari–Szabo model-free parameters, S^2 and τ_e, respectively. The conformational jumps of the CH_2 group, occurring on a slower time scale, are described by the two-site jump model. The two-site jump parameters (P, γ, and τ_j) and the model-free parameters were fitted simultaneously, together with one single common overall tumbling correlation time, τ_M. This global parameter provides the link between the two models. In practical implementation, Eqs. (3)–(6) are used for the data points identified as T_1, T_2 or NOE, whereas Eqs. (9)–(12) are employed for the CCRRs. All parameters and their uncertainties obtained in the simultaneous fit, according to the proposed method, are given in Table 3. The new results show that the integrated dynamic model even improves the quality of the Lipari–Szabo parameters, decreasing their errors compared to those in Table 2. Moreover, this kind of simultaneous fit allows us to extract what we believe to be reliable two-site jump parameters from our limited CCRRs. Attempts to calculate the two-site jump parameters exclusively from CCRRs (4 parameters from 4 measurables) were less successful even with the constraints of the global correlation times shown in Table 2.

The results, collected in Table 3, are promising. The global rotational correlation times and the S^2 order parameters are in a reasonable agreement with the results of the Lipari–Szabo model, cf. Table 2. The jump angle γ and population, P, are rather stable. The jump angle is in reasonable agreement with the results of Tvaroska et al. [48]. The most important results are the two-site jump rates, which are chemically the most interesting parameters. They are in the range 200–700 ps, not very different from the results of ultrasonic relaxation studies [49,50]. The jump rates increase, by and large, with the increasing temperature. The semilogarithmic Arrhenius plot of the jump rate versus inverse temperature for the range is

Table 3
Results of the combined dynamic model based on Lipari–Szabo fitting of T_1^{-1}, $T_{1\rho}^{-1}$, and NOE, and two-site jump fitting of $\Gamma_{CH,CH}^{long}$ and $\Gamma_{CH,CH}^{spin\text{-}lock}$ for the hydroxymethyl group in Me-β-D-glcp (all available experimental data were used at each temperature)

Temperature (K)	τ_M (ps)	P	γ (degree)	τ_j (ps)	S^2	τ_e (ps)
263	1657(95)	0.50(0.16)	62(8)	646(216)	0.79(0.02)	74(10)
277	677(29)	0.50(0.07)	52(8)	635(183)	0.81(0.02)	20(15)
284	535(42)	0.50(0.03)	50(5)	480(75)	0.73(0.04)	52(24)
300	416(245)	0.50(0.08)	51(5)	167(42)	0.50(0.23)	83(62)

The numbers in parentheses are parameter uncertainties estimated by a Monte Carlo procedure.

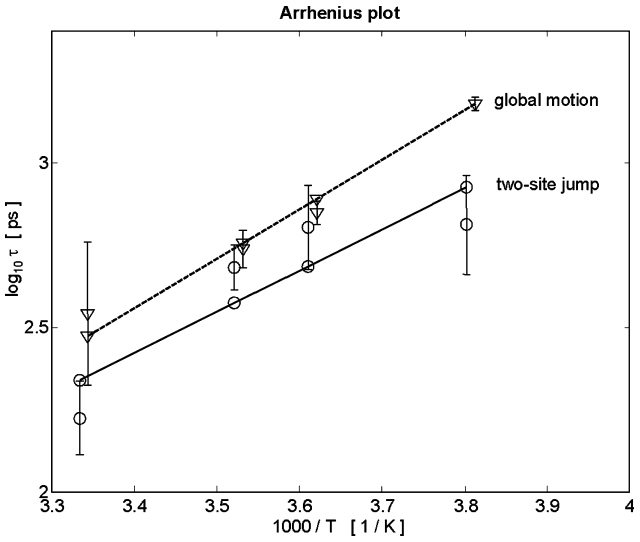

Fig. 6. Arrhenius plots of the inverse two-site jump rates (τ_j) and the global rotational correlation time (τ_M) according to Table 3. For better readability, the data for the global correlation time are shifted by 0.01 along the 1000/T axis.

shown in Fig. 6. The plot is reasonably linear and the derived activation energy, $E_a = 24 \pm 4\,\mathrm{kJ\,mol^{-1}}$, is in good agreement with ab initio calculation by Tvaroska et al. [48], who obtained the rotational barrier for methyl 2,3-dideoxy-β-D-glucopyranoside of about 25–30 kJ mol^{-1}. For the sake of comparison, we show in the same diagram also the corresponding plot for the global correlation time, which for sugar solutions is known to follow the Arrhenius relation [27,51].

5. Conclusions

We find in this study that the dipolar cross-correlated relaxation rates provide a suitable tool for selecting an appropriate model for conformational dynamics of hydroxymethyl groups in carbohydrates. For Me-β-D-glcp, we find that the two-site jump model can explain the sign and the magnitude of the CCRRs. The inverse jump rates (internal correlation times), based on the presented integrated approach of the auto- and cross-correlated relaxation data in Me-β-D-glcp, display reasonable temperature dependence. This study also emphasizes that cross-correlated relaxation data, combined with more traditional auto-correlated relaxation parameters, extend the possibilities for obtaining dynamic information that is difficult to obtain by other means.

Acknowledgments

This work has been supported by the Swedish Foundation for International Cooperation in Research and Education (STINT), the Royal Swedish Academy of Sciences and the Hungarian Academy of Science through grants supporting the visits of G.B. and K.K. in Stockholm. In addition, the support of the Swedish Research Council and of the Hungarian National Fund (OTKA T 042567 for G.B. and K.K.) is gratefully acknowledged. The authors are indebted to Prof. András Lipták and Dr. István Bajza for the sample of carbon-13 enriched Me-β-D-glcp and to Dr. Piotr Bernatowicz for assistance with some of the experiments.

References

[1] H. Shimizu, Theory of the dependence of nuclear magnetic relaxation on the absolute sign of spin–spin coupling constant, J. Chem. Phys. 40 (1964) 3357–3364.
[2] J.S. Blicharski, Interference effects in nuclear magnetic relaxation, Phys. Lett. A 24 (1967) 608–610.
[3] J.S. Blicharski, Interference effects in nuclear magnetic relaxation III, Acta Phys. Pol. A 38 (1970) 19–24.
[4] L.G. Werbelow, D.M. Grant, Intramolecular dipolar relaxation in multispin systems, Adv. Magn. Reson 9 (1977) 189–299.
[5] M. Goldman, Interference effects in the relaxation of a pair of unlike spin-1/2 nuclei, J. Magn. Reson. 60 (1984) 437–452.
[6] L.G. Werbelow, in: R. Tycko (Ed.), Nuclear Magnetic Probes of Molecular Dynamics, Plenum, New York, 1994, pp. 223–263.
[7] L.G. Werbelow, in: D.M. Grant, R.K. Harris (Eds.), Encyclopedia of Nuclear Magnetic Resonance, Wiley, Chichester, 1996, pp. 4072–4078.
[8] A. Kumar, R.C.R. Grace, P.K. Madhu, Cross-correlations in NMR, Prog. Nucl. Magn. Reson. Spectrosc. 37 (2000) 191–319.
[9] V.A. Daragan, K.H. Mayo, Motional model analyses of protein and peptide dynamics using C-13 and N-15 NMR relaxation, Prog. Nucl. Magn. Reson. Spectrosc. 31 (1997) 63–105.
[10] M.W.F. Fischer, A. Majumdar, E.R.P. Zuiderweg, Protein NMR relaxation: theory, applications and outlook, Prog. Nucl. Magn. Reson. Spectrosc. 33 (1998) 207–272.
[11] B. Brutscher, Principles and applications of cross-correlated relaxation in biomolecules, Concept Magn. Reson. 12 (2000) 207–229.
[12] D.M. Korzhnev, M. Billeter, A.S. Arseniev, V.Y. Orekhov, NMR studies of Brownian tumbling and internal motions in proteins, Prog. Nucl. Magn. Reson. Spectrosc. 38 (2001) 197–266.
[13] P. Luginbuhl, K. Wuthrich, Semi-classical nuclear spin relaxation theory revisited for use with biological macromolecules, Prog. Nucl. Magn. Reson. Spectrosc. 40 (2002) 199–247.
[14] D. Frueh, Internal motions in proteins and interference effects in nuclear magnetic resonance, Prog. Nucl. Magn. Reson. Spectrosc. 41 (2002) 305–324.
[15] A. Abragam, The Principles of Nuclear Magnetism, Oxford University Press, Oxford, 1961.
[16] D. Canet, Nuclear Magnetic Resonance: Concepts and Methods, Wiley, Chichester, 1996.
[17] V.A. Daragan, Different relaxation rates for separate lines in carbon-13 multiplets, Dokl. Akad. Nauk. SSSR 212 (1973) 657–659.
[18] V.A. Daragan, T.N. Khazanovich, A.U. Stepanyants, Cross-correlation effects in multiple spectra of carbon-13, Chem. Phys. Lett. 27 (1974) 89–92.
[19] D.M. Grant, C.L. Mayne, F. Liu, T.X. Xiang, Spin–lattice relaxation of coupled nuclear spins with applications to molecular motion in liquids, Chem. Rev. 91 (1991) 1591–1624.
[20] M. Ernst, R.R. Ernst, Heteronuclear dipolar cross-correlated cross relaxation for the investigation of side-chain motions, J. Magn. Reson. Ser. A 110 (1994) 202–213.

[21] J. Engelke, H. Rüterjans, Dynamics of β-CH and β-CH_2 groups of amino acid side chains in proteins, J. Biomol. NMR 11 (1998) 165–183.
[22] D. Yang, A. Mittermeier, Y.-K. Mok, L.E. Kay, A study of protein side-chain dynamics from new ^{2}H autocorrelation and ^{13}C cross-correlation experiments: application to the N-terminal SH3 domain from drk, J. Mol. Biol. 276 (1998) 939–954.
[23] D. Yang, Y.-K. Mok, D.R. Muhandiram, J.D. Forman-Kay, L.E. Kay, ^{1}H–^{13}C dipole–dipole cross-correlated spin relaxation as a probe of dynamics in unfolded proteins: application to the DrkN SH3 domain, J. Amer. Chem. Soc. 121 (1999) 3555–3556.
[24] L. Banci, I. Bertini, I.C. Felli, P. Hajieva, M.S. Viezzoli, Side chain mobility as monitored by CH–CH cross-correlation: the example of cytochrome b_5, J. Biomol. NMR 20 (2001) 1–10.
[25] M.T. Chenon, L.G. Werbelow, An NMR study of the solution dynamics of deltorphin-l, J. Amer. Chem. Soc. 124 (2002) 14066–14074.
[26] D.C. McCain, J.L. Markley, Internal motions of the three hydroxymethyl groups in aqueous sucrose, J. Magn. Reson. 73 (1987) 244–251.
[27] H. Kovacs, S. Bagley, J. Kowalewski, Motional properties of two disaccharides in solutions as studied by carbon-13 relaxation and NOE outside of the extreme narrowing region, J. Magn. Reson. 85 (1989) 530–541.
[28] J. Kowalewski, G. Widmalm, Multiple-field carbon-13 NMR relaxation study of cyclodextrins, J. Phys. Chem. 98 (1994) 28–34.
[29] L. Mäler, J. Lang, G. Widmalm, J. Kowalewski, Multiple-field carbon-13 NMR relaxation investigation on melezitose, Magn. Reson. Chem. 33 (1995) 541–548.
[30] J. Herzig, A. Nudelman, H.E. Gottlieb, Studies in sugar chemistry. Part V. Methanolysis of acetylated sugars and glycosides in the presence of tin oxides and alkoxides, Carbohydr. Res. 177 (1988) 21–28.
[31] J. Herzig, A. Nudelman, Studies in sugar chemistry. Part III. Regioselective heterogeneous O-deacylation of polyacylated sugars, Carbohydr. Res. 153 (1986) 162–167.
[32] C. Ammann, P. Meier, A.E. Merbach, A simple multinuclear NMR thermometer, J. Magn. Reson. 46 (1982) 319–321.
[33] J. Kowalewski, A. Ericsson, R. Vestin, Determination of NOE factors using the dynamic Overhauser enhancement technique combined with a non-linear fitting procedure, J. Magn. Reson. 31 (1978) 165–169.
[34] K.E. Kövér, G. Batta, Simple difference experiments for detection of cross-correlation, Appl. Magn. Reson. 2 (1991) 729–740.
[35] G. Jaccard, S. Wimperis, G. Bodenhausen, Observation of $2I_zS_z$ order in NMR relaxation studies for measuring cross-correlation of chemical shift anisotropy and dipolar interactions, Chem. Phys. Lett. 138 (1987) 601–606.
[36] MATLAB 5.3 Reference Guide, Math Works, Natick, MA.
[37] D. Doddrell, V. Glushko, A. Allerhand, Theory of nuclear Overhauser enhancement and carbon-13–proton dipolar relaxation in proton-decoupled carbon-13 NMR spectra of macromolecules, J. Chem. Phys. 56 (1972) 3683–3689.
[38] J. Brondeau, D. Canet, Longitudinal magnetic relaxation of carbon-13 (or nitrogen-15) interacting with a strongly irradiated proton system, J. Chem. Phys. 67 (1977) 3650–3654.
[39] G. Lipari, A. Szabo, Model-free approach to the interpretation of nuclear magnetic resonance relaxation in macromolecules 1. Theory and range of validity, J. Amer. Chem. Soc. 104 (1982) 4546–4559.
[40] L.Y. Zhu, M.D. Kemple, S.B. Landy, P. Buckley, Effect of dipolar cross correlation on model-free motional parameters obtained from C-13 relaxation in AX2 systems, J. Magn. Reson. Ser. B 109 (1995) 19–30.
[41] L.E. Kay, D.A. Torchia, The effects of dipolar cross correlation on C-13 methyl–carbon T1, T2, and NOE measurements in macromolecules, J. Magn. Reson. 95 (1991) 536–547.
[42] V.A. Daragan, K.H. Mayo, Using the model-free approach to interpret C-13 NMR multiplet relaxation data from peptides and proteins, J. Magn. Reson. Ser. B 107 (1995) 274–278.
[43] Y. Ishii, T. Terao, S. Hayashi, Theory and simulation of vibrational effects on structural measurements in solid-state NMR, J. Chem. Phys. 107 (1997) 2760–2774.
[44] J. Kowalewski, M. Effemey, J. Jokisaari, Dipole–dipole coupling constant for a directly bonded CH pair—a carbon-13 relaxation study, J. Magn. Reson. 157 (2002) 171–177.
[45] M. Ottiger, A. Bax, Determination of relative N–HN, N–C′, C-alpha-C′, and C(Alpha)-H-alpha effective bond lengths in a protein by NMR in a dilute liquid crystalline phase, J. Amer. Chem. Soc. 120 (1998) 12334–12341.
[46] C.A.G. Haasnoot, F.A.A.M. DeLeeuw, C. Altona, The relation between proton–proton NMR coupling constants and substituent electronegativities. I. An empirical generalization of the Karplus equation, Tetrahedron 36 (1980) 2783–2792.
[47] R. Stenutz, I. Carmichael, G. Widmalm, A. Serianni, Hydroxymethyl group conformation in saccharides: structural dependencies of 2JHH, 3JHH, and 1JCH spin–spin coupling constants, J. Org. Chem. 67 (2002) 949–958.
[48] I. Tvaroska, F.R. Taravel, J.P. Utille, J.P. Carver, Quantum mechanical and NMR spectroscopy studies on the conformations of the hydroxymethyl and methoxymethyl groups in aldohexosides, Carbohydr. Res. 337 (2002) 353–367.
[49] R. Behrends, M.K. Cowman, F. Eggers, E.M. Eyring, U. Kaatze, J. Majewski, S. Petrucci, K.-H. Richmann, M.J. Riech, Ultrasonic relaxation and fast chemical kinetics of some carbohydrate aqueous solutions, J. Amer. Chem. Soc. 119 (1997) 2182–2186.
[50] J. Stenger, M. Cowman, F. Eggers, E.M. Eyring, U. Kaatze, S. Petrucci, Molecular dynamics and kinetics of monosaccharides in solution. A broadband ultrasonic relaxation study, J. Phys. Chem. B 104 (2000) 4782–4790.
[51] G. Batta, K.E. Kövér, J. Gervay, M. Hornyák, G.M. Roberts, Temperature dependence of molecular conformation, dynamics, and chemical shift anisotropy of alpha,alpha-trehalose in D_2O by NMR relaxation, J. Amer. Chem. Soc. 119 (1997) 1336–1345.